

Short Wave Infrared Neuromodulation Gadget

Cameron R. Author, *Member, IEEE*, Matthew T. Author, Bibhus L. Author, Krishna S. Sponsor, *Member, IEEE*, John L. Mentor, *Member, IEEE*

Abstract—Direct stimulation of neurons in the brain can potentially treat many diseases, such as Parkinson’s or Alzheimer’s disease. Direct stimulation, whether it be through electric or photonic stimulation, provided a way to activate neurons in the brain and treat diseases and conditions. However, this kind of invasive stimulation can have risks that lead to worsening the condition or cause infection. The Short-Wave Infrared Neuromodulation Gadget (SWING) aimed to build and test a non-invasive optical method of stimulation with funding provided by the KIND Laboratory’s Brain IMPACT project. SWING is part of the two semester long Electrical and Computer Engineering capstone sequence at The Ohio State University.

SWING used a cubic extrapolation to approximate the optical coefficients of biological tissue at 1550 nm. Monte Carlo eXtreme (MCX) was then used to predict the expected photon distribution and intensity throughout a model of the human head. MCX was ran multiple times with different positions and wavelengths using The Ohio State Supercomputer. MCX showed that deep brain stimulation is possible at all the wavelengths tested. Based on the MCX results, 1550nm wavelength is the most compelling choice for further testing.

Index Terms—

I. INTRODUCTION

HERE are many physical issues in the brain, including Parkinson’s disease and functional problems such as attention-deficit/hyperactivity disorder (ADHD) and depressive disorders. A solution to such problems that has been explored recently in the Neurotech community is one that involves a direct stimulation of neuronal connections in the brain [1]–[3]. Direct neuronal stimulation, whether it be through electric or photonic stimulation, provides a way to control mechanisms in the brain and treat diseases and conditions. These treatments result in an improvement of the effects caused by these diseases and conditions. However, most modern neuromodulation strategies are invasive in nature, and there are limited options for a non-invasive approach to neuromodulation for medical benefit. Many invasive techniques involve surgical implants and increase the risk of brain hemorrhage and worsening mental and emotional status for some patients, that often make the cons worse for life-threatening conditions [1], [4]. As a result, the Short-Wave Infrared Neuromodulation Gadget (SWING) looks to investigate a non-invasive method for neuromodulation using a near-infrared photonic stimulation method.

II. METHODS

SWING’s software and simulation consisted of two main components: software for data preprocessing and simulation for modeling and photon distribution. The preprocessing stage involved approximating optical coefficients at 1550 nm.. Monte Carlo eXtreme (MCX) is used for simulating the behavior of the laser as it scatters and is absorbed through brain tissue, providing a model of photon dispersion in biological tissue using known or approximated optical coefficients.

A. Software Preprocessing

In the software preprocessing stage, the model approximated the optical coefficients of layers in the brain where it is unknown for 1550nm sources. Optical coefficient data for the scalp, skull, gray matter (GM), and white matter (WM) are obtained from [SOURCE]. The wavelength ranges for each layer are as follows: scalp (805-2000 nm), skull (801-2000 nm), gray matter (400-1300 nm), and white matter (400-1300 nm). The data for scalp and skull cover the wavelength of interest (1550 nm), but the data for GM and WM do not. To address this, cubic extrapolation and interpolation methods are used to process the data and extrapolate the unknown layers to 1550nm.

The cubic interpolation method approximates the optical coefficients for the gray matter (GM) and white matter (WM) layers at 1550 nm based on the known data points. Let x represent the wavelength and y represent the absorption coefficient. The cubic interpolation function can be defined as follows:

$$y(x) = a(x - x_1)^3 + b(x - x_1)^2 + c(x - x_1) + d$$

where (x_1, y_1) , (x_2, y_2) , (x_3, y_3) , and (x_4, y_4) are the known data points for a specific layer (GM or WM).

To determine the coefficients a , b , c , and d , the model solves the following system of equations using the known data points:

$$\begin{aligned} y_1 &= a(x_1 - x_1)^3 + b(x_1 - x_1)^2 + c(x_1 - x_1) + d \\ y_2 &= a(x_2 - x_1)^3 + b(x_2 - x_1)^2 + c(x_2 - x_1) + d \\ y_3 &= a(x_3 - x_1)^3 + b(x_3 - x_1)^2 + c(x_3 - x_1) + d \\ y_4 &= a(x_4 - x_1)^3 + b(x_4 - x_1)^2 + c(x_4 - x_1) + d \end{aligned}$$

Solving this system of equations provides the coefficients a , b , c , and d specific to the cubic interpolation for the respective layer.

To apply the cubic interpolation in this study, Python programming language was used to process the known data

points and calculate the coefficients. Once the coefficients are obtained, the cubic interpolation function is used to estimate the absorption coefficient at any desired wavelength within the range. This cubic interpolation provides a complex fit while preventing over-fitting in the initial steps. This allows extrapolation of the gray and white matter absorption coefficients to 1550 nm within the overlapping region (801-1300 nm), providing continuous lines for the unknown layers.

To extrapolate the optical coefficients of the gray matter (GM) and white matter (WM) layers to 1550 nm, the overlapping region of the four tissues (801-1300 nm) is examined. Vertical offset values between the unknown layers (GM and WM) and the known layers (scalp and skull) are calculated throughout this overlapping region.

Let λ represent the wavelength and μ represent the absorption coefficient. The vertical offset values can be calculated as the difference between the absorption coefficients of the unknown layers and the known layers at each wavelength in the overlapping region. These offset values are averaged to obtain two average vertical offsets, one for each unknown layer. Let AvgOffsetGM represent the average vertical offset of the gray matter, and AvgOffsetWM represent the average vertical offset of the white matter. The extrapolation model then extends the unknown layers by adding the previously calculated offsets to the known scalp and skull data.

The average vertical offsets of the gray matter and white matter can be expressed as:

$$\text{AvgOffsetGM} = \frac{1}{N} \sum_{i=1}^N (\mu_{\text{GM,unknown}}(\lambda_i) - \mu_{\text{GM,known}}(\lambda_i))$$

$$\text{AvgOffsetWM} = \frac{1}{N} \sum_{i=1}^N (\mu_{\text{WM,unknown}}(\lambda_i) - \mu_{\text{WM,known}}(\lambda_i))$$

where N represents the number of data points within the overlapping region, $\mu_{\text{GM,unknown}}(\lambda_i)$ and $\mu_{\text{WM,unknown}}(\lambda_i)$ denote the absorption coefficients of the unknown layers at the i -th wavelength, and $\mu_{\text{GM,known}}(\lambda_i)$ and $\mu_{\text{WM,known}}(\lambda_i)$ denote the absorption coefficients of the known layers at the i -th wavelength.

In this study, Python programming language was used to process the absorption coefficient data and calculate the vertical offset values. The following equations were used to perform the extrapolation:

$$\mu_{\text{GM,extrapolated}}(\lambda) = \mu_{\text{GM,known}}(\lambda) + \text{AvgOffsetGM}$$

$$\mu_{\text{WM,extrapolated}}(\lambda) = \mu_{\text{WM,known}}(\lambda) + \text{AvgOffsetWM}$$

To ensure accuracy and account for variations, this process of calculating vertical offsets and performing extrapolation is repeated for multiple data points within the overlapping region.

Figures 7, 8, and 9 visualize the results of the extrapolation process. Figure 7 shows the overlapping region of absorption coefficients, and Figures 8 and 9 display the extrapolated absorption coefficients at 1550 nm. These figures, generated using Python, provide a graphical representation of the extrapolation results and aid in understanding the estimated optical

coefficients of the GM and WM layers at the wavelength of interest.

B. Simulation using MCX

MCX, a Monte Carlo simulation tool, is employed for visualizing the optical intensity and behavior of a laser source within the head and brain tissue. It models the photon dispersion in biological tissue using optical coefficients obtained from experimental data or approximations, as in the case of SWING. MCX creates a mesh model of the human brain using an accumulation of MRI images, incorporating layers such as scalp, skull, Cerebral Spinal Fluid (CSF), GM, WM, and air bubbles. Thickness variations in the layers are specified using thinning or thickening operators. To create the simulation, the optical coefficients, particularly the absorption and scattering coefficients, are input into the MCX software. This allows for the simulation of photon absorption and scattering as light passes through the brain tissue, enabling visualization of beam intensity at different points in the brain. Additionally, SWING utilizes the software to investigate various aspects of photon dispersion. This includes studying the impact of different tissue layers on beam intensity and exploring the effects of laser parameters such as wavelength, illumination area size, and the number of incident photons on the phantom. The differences between absorption coefficients at 1550 nm compared to other wavelength be observed and noted in the figures, and this model can be utilized for experimental data validation.

III. RESULTS

Table I displays the estimated absorption and scattering coefficients for each of the biological tissue layers as well as each wavelength. These values were calculated using the interpolation-extrapolation method detailed in Section II. To determine the reliability of this prediction method, SWING used the Python library "scikit-learn" to calculate the R-squared value when predicting known data. This R-squared value was calculated as 0.4980, indicating that 49.80% of the variability in the unknown coefficients is explained by SWING's prediction model.

IV. DISCUSSION

V. CONCLUSION

ACKNOWLEDGMENT

REFERENCES

- [1] "Novel Neuromodulation Techniques," in *IEEE Pulse*, Aug. 2016. <https://www.embs.org/pulse/articles/novel-neuromodulation-techniques/>
- [2] "Improvements in clinical signs of Parkinson's disease using photobiomodulation: a prospective proof-of-concept study," in *BMC Neurology*, Jul. 2021. <https://www.embs.org/pulse/articles/novel-neuromodulation-techniques/>
- [3] "Deep Brain stimulation," in *Mayo Clinic*, Sep. 2021. <https://www.mayoclinic.org/tests-procedures/deep-brain-stimulation/about/pac-2038456>
- [4] C. C. medical professional, "Deep Brain Stimulation (DBS): What it is, Purpose & procedure," in *Cleveland Clinic*, <https://my.clevelandclinic.org/health/treatments/21088-deep-brain-stimulation#risks-ben>

TABLE I
ESTIMATED OPTICAL COEFFICIENTS

Tissue Type	Wavelength, nm	Absorption Coefficient μ_a , cm^{-1}	Scattering Coefficient μ_s' , cm^{-1}
Scalp	810	0.505	14.145
	980	0.365	16.714
	1064	0.168	17.029
	1550	1.649	14.578
Skull	810	0.099	19.248
	980	0.230	17.380
	1064	0.101	16.180
	1550	2.715	15.543
Gray Matter	810	[0.455,0.605,0.744]	[3.896,6.030,8.211]
	980	[0.586,0.601,0.610]	[6.343,6.380,6.444]
	1064	[0.413,0.438,0.457]	[5.143,5.938,6.740]
	1550	[1.870,2.485,3.071]	[4.246,4.393,4.506]
White Matter	810	[0.737,0.888,1.027]	[24.237,26.403,28.617]
	980	[0.868,0.883,0.893]	[26.749,26.753,26.785]
	1064	[0.696,0.720,0.739]	[25.549,26.311,27.081]
	1550	[2.153,2.767,3.353]	[24.587,24.767,24.911]

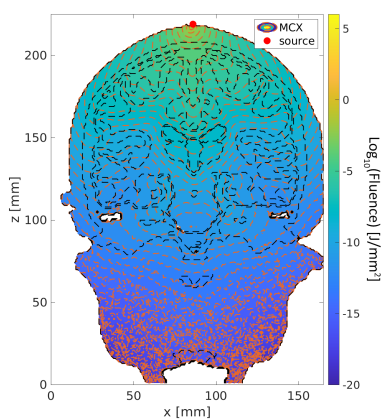


Fig. 1. 810 nm CZ Position

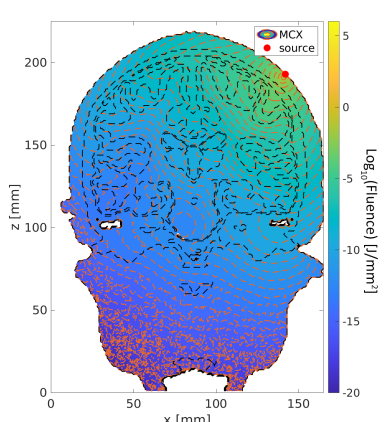


Fig. 2. 810 nm 45 Degree Position

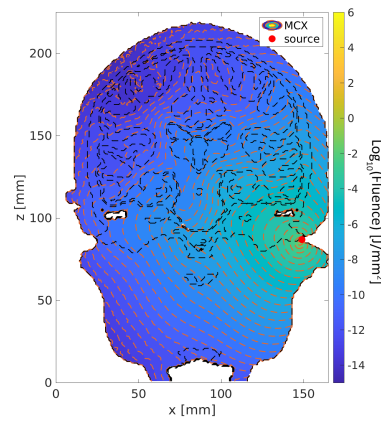


Fig. 3. 810 nm Cochlear Position

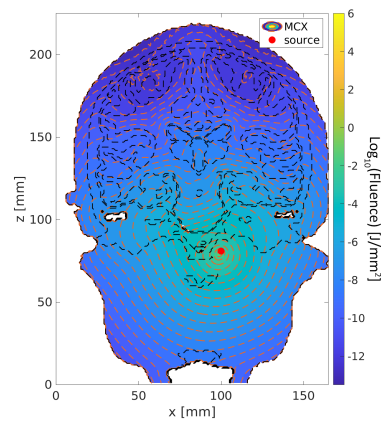


Fig. 4. 810 nm Intranasal Position

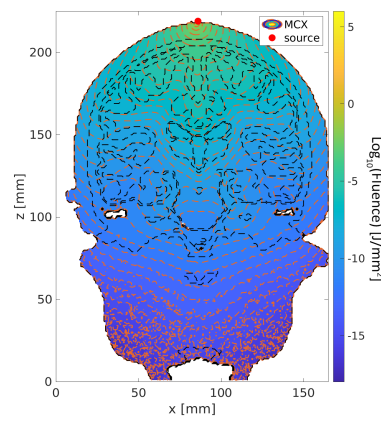


Fig. 5. 980 nm CZ Position

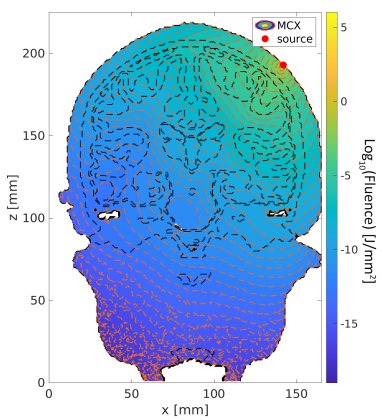


Fig. 6. 980 nm 45 Degree Position

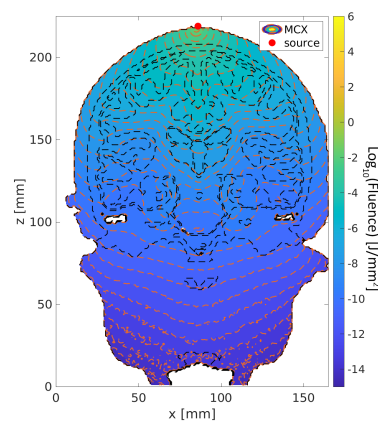


Fig. 9. 1064 nm CZ Position

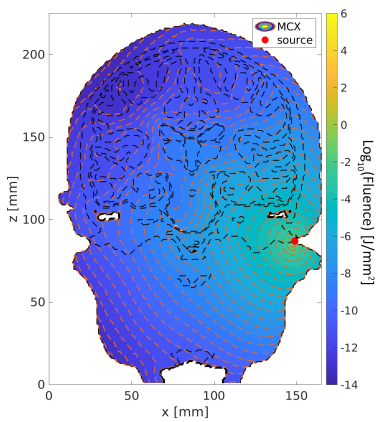


Fig. 7. 980 nm Cochlear Position

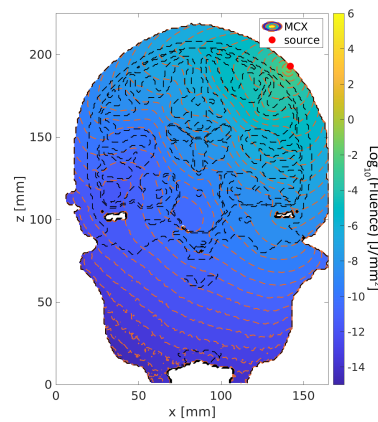


Fig. 10. 1064 nm 45 Degree Position

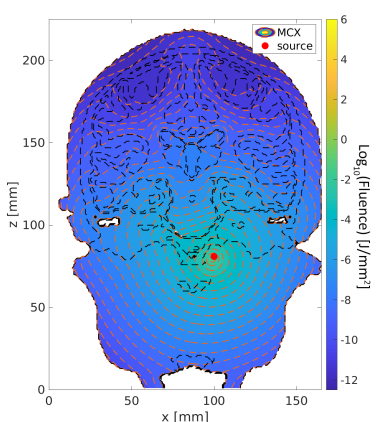


Fig. 8. 980 nm Intranasal Position

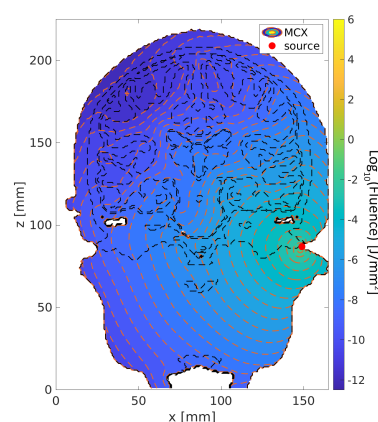


Fig. 11. 1064 nm Cochlear Position

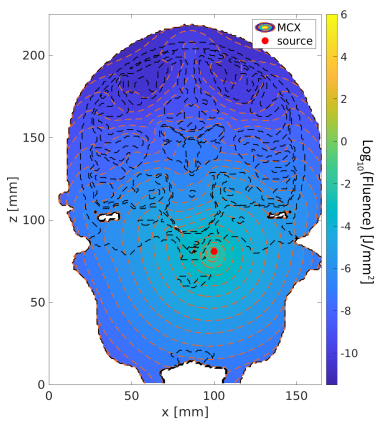


Fig. 12. 1064 nm Intransal Position

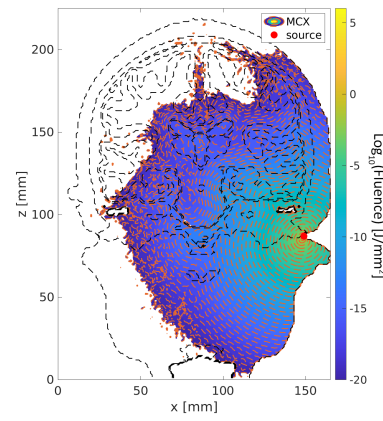


Fig. 15. 1550 nm Cochlear Position

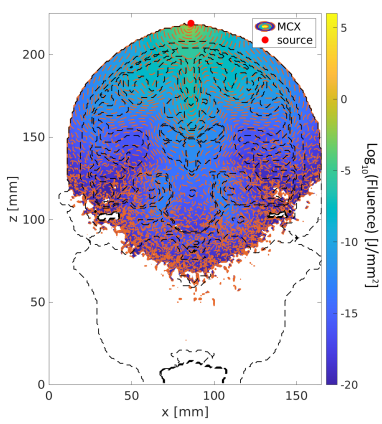


Fig. 13. 1550 nm CZ Position

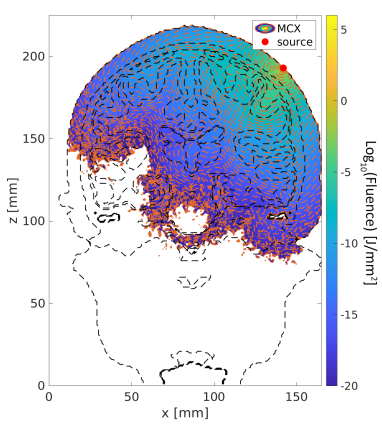


Fig. 14. 1550 nm 45 Degree Position

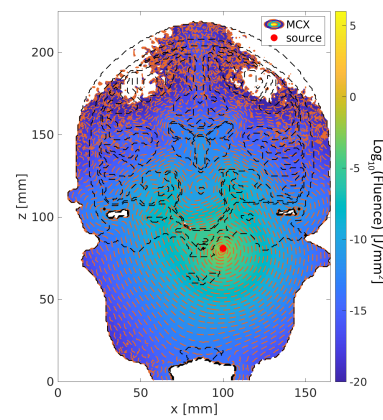


Fig. 16. 1550 nm Intransal Position